

UC Berkeley

UC Berkeley Previously Published Works

Title

Chemoproteomics-Enabled Covalent Ligand Screening Reveals a Thioredoxin-Caspase 3 Interaction Disruptor That Impairs Breast Cancer Pathogenicity

Permalink

<https://escholarship.org/uc/item/1b65450c>

Journal

ACS Chemical Biology, 12(10)

ISSN

1554-8929

Authors

Anderson, Kimberly E
To, Milton
Olzmann, James A
et al.

Publication Date

2017-10-20

DOI

10.1021/acscchembio.7b00711

Peer reviewed



HHS Public Access

Author manuscript

ACS Chem Biol. Author manuscript; available in PMC 2018 October 29.

Published in final edited form as:

ACS Chem Biol. 2017 October 20; 12(10): 2522–2528. doi:10.1021/acscchembio.7b00711.

Chemoproteomics-Enabled Covalent Ligand Screening Reveals a Thioredoxin-Caspase 3 Interaction Disruptor That Impairs Breast Cancer Pathogenicity

Kimberly E. Anderson^{†,‡}, Milton To[‡], James A. Olzmann[‡], and Daniel K. Nomura^{*,†,‡}

[†]Departments of Chemistry, Molecular and Cell Biology, University of California, Berkeley, Berkeley, California 94720, United States

[‡]Departments of Nutritional Sciences and Toxicology, University of California, Berkeley, Berkeley, California 94720, United States

Abstract

Covalent ligand discovery is a promising strategy to develop small-molecule effectors against therapeutic targets. Recent studies have shown that dichlorotriazines are promising reactive scaffolds that preferentially react with lysines. Here, we have synthesized a series of dichlorotriazine-based covalent ligands and have screened this library to reveal small molecules that impair triple-negative breast cancer cell survival. Upon identifying a lead hit from this screen KEA197, we used activity-based protein profiling (ABPP)-based chemoproteomic platforms to identify that this compound targets lysine 72 of thioredoxin—a site previously shown to be important in protein interactions with caspase 3 to inhibit caspase 3 activity and suppress apoptosis. We show that KEA1–97 disrupts the interaction of thioredoxin with caspase 3, activates caspases, and induces apoptosis without affecting thioredoxin activity. Moreover, KEA1–97 impairs *in vivo* breast tumor xenograft growth. Our study showcases how the screening of covalent ligands can be coupled with ABPP platforms to identify unique anticancer lead and target pairs.

Abstract Graphic

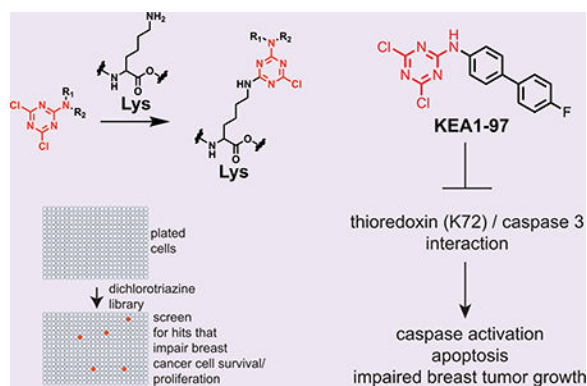
*Corresponding Author: dnomura@berkeley.edu.

Notes

The authors declare no competing financial interest.

Supporting Information

The Supporting Information is available free of charge on the ACS Publications website at DOI: 10.1021/acscchembio.7b00711.



Searching for novel cancer targets often involves hunting for genes or proteins that may be mutated or upregulated in tumors. However, this strategy may neglect cancer therapy targets that may not possess altered activity or expression. Screening small-molecule libraries for compounds that impair cancer pathogenicity in chemical genetics screens has arisen as a powerful complementary platform to traditional target discovery approaches for identifying new drugs that may target unique proteins for cancer therapy.^{1,2} A major challenge with chemical genetics, however, is identifying the protein targets of screening hits. Hits from screens must usually be derivatized with analytical handles for enrichment and proteomic identification of targets, which necessitate altering the structure of the molecule, which may affect its activity and hinder target identification.³

Isotopic tandem orthogonal proteolysis-enabled activitybased protein profiling (isoTOP-ABPP) is one such chemoproteomic strategy that overcomes many of these challenges.⁴⁻⁶ IsoTOP-ABPP uses reactivity-based chemical probes to map reactive and druggable hotspots directly in complex proteomes. This platform can be used in a competitive mode to compete covalently acting small molecules against a reactivity-based probe binding to ligandable sites in the proteome to facilitate both rapid target discovery as well as the identification of druggable hotspots targeted by covalent ligands. Recent studies have shown the promise of coupling covalent ligand discovery using cysteine-reactive ligand libraries with competitive isoTOP-ABPP platforms to facilitate the discovery of small molecules that target unique and novel druggable hotspots in complex biological systems.⁵⁻⁷ Studies using this coupled approach have primarily focused thus far on cysteine reactivity. However, recent studies have shown that other reactive scaffolds targeting other amino acids may also be used in combination with chemoproteomic platforms to discover unique and novel druggable hotspots in proteins.⁸⁻¹¹ Among these scaffolds, dichlorotriazines have been demonstrated to show preference for lysines, and this scaffold can also be used as a reactivity-based probe for chemoproteomic studies.⁸

In this study, we coupled the screening of a dichlorotriazinebased covalent ligand library with isoTOP-ABPP platforms to identify compounds and druggable hotspots that impair the pathogenicity of triple-negative breast cancer (TNBC) cells, a subset of breast cancers devoid of estrogen, progesterone, and HER2 receptors. TNBCs show the worst prognosis due to the lack of targeted therapies available. We synthesized 58 dichlorotriazine-based covalent ligands and screened this library to identify hits that impaired 231MFP TNBC

serum-free cell survival and serum-containing cell proliferation (Supporting Methods, Figure 1A–C; Figure S1, Table S1). We then counterscreened any hits that showed >50% reductions in either survival or proliferation against MCF10A nontransformed epithelial cells to ensure that any lead hits did not cause nonspecific cytotoxicity (Figure 1D; Figure S1, Table S1). Through this screening effort, we identified a hit KEA1–97 that impaired 231MFP cell survival and proliferation and does not affect viability in MCF10A cells (Figures 1A–C and 2A).

We next performed competitive isoTOP-ABPP with KEA197 *in vitro* against a dichlorotriazine-alkyne probe (DCTalkyne) in 231MFP proteomes to identify specific targets of KEA1–97. We preincubated KEA1–97 or vehicle with 231MFP proteomes prior to labeling of proteomes with DCT-alkyne, followed by copper-catalyzed alkyne azide cycloaddition (CuAAC)-mediated appendage of a biotin-azide tag bearing an isotopically light or heavy mass tag with a TEV protease recognition site for vehicle or KEA1–97-treated proteomes, respectively. Vehicle and covalent ligand-treated proteomes were then combined in a 1:1 ratio. Probe-labeled proteins were avidin-enriched and tryptically digested, and probe-modified tryptic peptides were isolated and eluted by TEV protease for subsequent quantitative proteomic analysis. We then quantified isotopically light to heavy probe-modified peptide ratios, where a ratio of ~1 indicated no binding by KEA1–97, whereas a ratio >10 indicated a target of KEA1–97. We identified the primary target of KEA1–97 as lysine 72 (K72) of thioredoxin (TXN), showing an isotopically light to heavy peptide ratio of 38 (Figure 2A; Table S2). The interaction between KEA1–97 and TXN was validated through fluorescent gel-based ABPP detection showing competition of KEA1–97 against DCTalkyne labeling of pure human TXN with a 50% inhibitory concentration of 10 μ M (Figure 2B). To further demonstrate that TXN was involved in the antisurvival and antiproliferative effects of KEA1–97, we tested whether KEA1–97 effects were attenuated upon stable overexpression of TXN in 231MFP breast cancer cells. We showed that 2.5-fold higher TXN expression in 231MFP cells led to a significant resistance to survival and proliferation impairments induced by KEA1–97 (Figure 2C,D). We further demonstrated that the dichlorotriazine reactive warhead is necessary for KEA1–97 interactions with TXN. Replacement of the dichlorotriazine in KEA1–97 with an unreactive dimethoxytriazine (KEA1–146) group prevented binding to pure human TXN protein and failed to impair cell survival and proliferation of 231MFP cells (Figure S2). Longer incubation times with KEA1–97 could also lead to increased nonspecific reactivity with protein targets. However, we did not observe this as assessed by gel-based ABPP methods in 231MFP proteomes (Figure S2). In addition, to further test the proteome-wide selectivity for KEA1–97, we also performed isoTOP-ABPP studies competing KEA1–97 against our recently disclosed NHS-ester-alkyne reactivity-based probe.¹⁰ Interestingly, while this probe identified >1000 probe-modified lysines in 231MFP cells, compared to the 80 lysines profiled by the DCT-alkyne probe, we did not identify K72 of TXN. Rather, the NHS-ester-alkyne probe labeled K94 of TXN which showed an isotopically light to heavy ratio of 1.0, indicating that this site was not a target of KEA1–97. Across >1000 profiled lysines with the NHS-ester probe, there were no targets that showed a ratio >3, demonstrating the remarkable selectivity of KEA1–97 for K72 of TXN in 231MFP cell proteomes (Figure S3, Table S2).

Interestingly, a previous study showed that K72 is a critical residue for interaction of thioredoxin with procaspase 3. Upon interaction, thioredoxin nitrosylates the active-site cysteine of procaspase 3 to inhibit its activity and suppress apoptosis.¹² We found that KEA1–97 does not inhibit TXN activity—an expected result because KEA1–97 is not binding to the active site (Figure 2E). Consistent with the role of K72 in protein interactions, we showed that TXN pulldown of caspase 3 using pure proteins is impaired by KEA1–97 treatment (Figure 2F). We further demonstrate that caspase 3 interactions with TXN are also significantly disrupted upon mutation of K72 on TXN to an alanine (Figure 2F). From these results, we expected that disrupting the interactions between TXN and caspase 3 with KEA1–97 would lead to activation of caspase 3 and induction of apoptosis. Consistent with this premise, KEA1–97 treatment in 231MFP cells activated caspase 3/7 and induced apoptotic cell death (Figure 3A,B). We next investigated whether this pro-apoptotic effect of KEA1–97 upon TNBC cells may translate to in vivo antitumorigenic effects in mice. KEA1–97 daily in vivo treatments (5 mg/kg ip) started after tumor establishment significantly attenuated tumor xenograft growth of 231MFP breast cancer cells in immune-deficient mice without causing any overt toxicity (Figure 3C).

We thus showed in this study that screening of lysine-reactive covalent ligand libraries can be coupled with isoTOP-ABPP platforms to discover new leads, targets, and druggable hotspots for combatting TNBC pathogenicity. In particular, we showed here that apoptosis of TNBC cells can be induced by disrupting a protein–protein interaction between TXN and caspase 3 through targeting K72 of TXN with the dichlorotriazine covalent ligand KEA1–97. While we cannot exclude additional mechanisms that may contribute to the anticancer activity of KEA1–97, we show that KEA1–97 selectively modulates certain functions of TXN through protein interactions with caspase 3 without affecting its catalytic activity. Targeting this unique druggable hotspot may therefore be a safer approach for targeting thioredoxin for cancer rather than inhibiting its many other activities in repairing oxidized cysteines or disulfides in proteins. We demonstrate that there appears to be a modest therapeutic window in which KEA1–97 impairs 231MFP TNBC survival and proliferation without significantly affecting nontransformed MCF10A cell viability and that KEA1–97 daily treatment at 5 mg/kg ip is well-tolerated in mice. However, future studies should be performed to elucidate the safety and toxicity profile of KEA1–97 prior to its development as a breast cancer therapeutic.

Overall, our study showcases a pipeline for coupling phenotypic screening of lysine-reactive small-molecule libraries with chemoproteomic platforms to rapidly discover lead small molecules that target unique and novel druggable hotspots for disease therapy. Our group as well as Backus and others have previously shown the utility of these approaches with cysteinereactive covalent ligands.^{6,7,13} More recently, we reported an even broader NHS-ester-alkyne chemoproteomics-compatible reactivity-based probe that reacts primarily with lysines, but also with serines, threonines, tyrosines, and other amino acids, where we showed that the reactivity of NHS-ester-based covalent ligands can be tuned to selectively target certain proteins.¹⁰ Hacker and colleagues have also reported multiple lysine-selective chemoproteomic probes for profiling >9000 lysines in complex proteomes and identify lysine-reactive covalent ligands that selectively and uniquely modulate protein functions through binding allosteric sites as well as protein–protein interaction sites.⁹ Zhao and

colleagues have also revealed sulfonyl fluorides as a scaffold for targeting lysines, particularly within kinase ATP binding sites.¹⁴ Lin and colleagues also recently reported on oxaziridines as chemoselective probes for methionines.¹¹ Expansion of both chemoproteomic probes and associated covalent ligand libraries targeting cysteines, lysines, methionines, and other amino acids will undoubtedly lead to rapid advancements in the future discovery of novel druggable hotspots and targets that can be pharmacologically targeted for drug discovery efforts.

■ METHODS

Materials

DCT-alkyne was synthesized as previously reported.⁸ A description of NHS-ester-alkyne was previously reported.¹⁰ Synthetic methods and characterization of the dichlorotriazine library is reported in the Supporting Information.

Cell Culture

Professor Benjamin Cravatt's group provided the 231MFP cells. MCF10A cells were purchased from ATCC. 231MFP and MCF10A cells were cultured as previously reported.^{15,16}

Survival and Proliferation Assays

Cells were plated the evening before the experiment and allowed to adhere overnight. For serum-free cell survival assays, cells were plated in media not containing FBS. For cell proliferation assays, cells were plated in complete media. For the chemical genetics screen, cells were treated with either ACN or the lysine-reactive fragment for 48 h at 10 μ M, and cell viability was assessed by Hoechst stain using our previously described methods.¹⁶

Tumor Xenograft Growth Studies

C.B17 SCID male mice (6–8 weeks old) were injected subcutaneously into the flank with 2 000 000 cells in serum-free media. For pharmacological treatments, mice were exposed by intraperitoneal (ip) injection with either vehicle (18:1:1 PBS/ethanol/PEG40) or 5 mg/kg KEA1–97 once per day starting 16 days after the initiation of the xenograft experiment and until the completion of the study. Tumors were measured roughly every 7 days by caliper measurements. Animal experiments were conducted in accordance with the guidelines of the Institutional Animal Care and Use Committee of the University of California, Berkeley.

IsoTOP-ABPP Analysis

IsoTOP-ABPP analyses were performed as previously described.^{6,17,18} For competitive IsoTOP-ABPP, 231MFP cell lysates were preincubated with acetonitrile (ACN) vehicle or KEA1–97 (10 μ M) for 30 min at 37 °C in phosphatebuffered saline (PBS) and then labeled with DCT-alkyne (100 μ M) or NHS-ester-alkyne (500 μ M) for 1 h at RT. Lysates were then treated with isotopically light (control) or heavy (treated) TEV-biotin (100 μ M), and CuAAC was performed as previously reported.^{13,19} Subsequent steps of the isoTOP-ABPP and mass

spectrometry procedures were performed using the same methods as we have previously described.^{13,19}

Peptides were searched with a static modification for cysteine carboxyamino-methylation (+57.02146) and up to two differential modifications for methionine oxidation and lysine probe modifications with either the light or heavy TEV tags—+550.22797 or +556.24178, respectively, for the DCT-alkyne probe and +494.26013 or +500.27394, respectively, for the NHS-ester-alkyne probe. Peptides were required to have at least one tryptic end and to contain the TEV modification. ProLUCID data were filtered through DTASelect to achieve a peptide false-positive rate below 1%.

Gel-Based ABPP

These experiments were achieved as previously described.^{13,19} Recombinant thioredoxin (0.04 μg) protein was pretreated with ACN or KEA1-97, respectively, for 30 min at 37 °C in an incubation volume of 50 μL of PBS and were subsequently treated with DCT-alkyne (100 μM final concentration) for 30 min at 37 °C. Rhodamine-azide was appended by CuAAC onto DCT-alkyne probe-labeled proteins. The samples were separated by SDS/PAGE and analyzed for in-gel fluorescence.

Ni-NTA Magnetocapture Assay

Recombinant his-tagged TXN (Enzo Life Sciences Inc., ADI-SPP-892-200) was used as bait to precipitate pure recombinant caspase-3 (Origene Technologies Inc., TP304444) using Ni-NTA magnetic agarose beads (Qiagen, 220002-020). One microgram of His-txn was added to 50 μL of binding buffer (25 mM NaH_2PO_4 /250 mM NaCl/10 mM imidazole/5% vol/vol glycerol/0.05 wt %/wt CHAPS, pH 8.0), followed by the addition of KEA1-97 (100 μM final concentration) or equivalent volume of acetonitrile. Samples were incubated at 37 °C for 30 min with shaking. One microgram of pure caspase 3 was added to each sample, and samples were incubated at 37 °C for 30 min with shaking. Twenty microliters of Ni-NTA magnetic agarose beads were added to each sample, and samples were rotated at 4 °C for 2 h. Washes (3 times, 1 mL binding buffer) were performed using a New England BioLabs magnetic separation rack. The proteins were eluted using 20 μL of binding buffer supplemented with imidazole to a final concentration of 0.5 M. After the addition of Laemmli's reducing agent, samples were boiled at 95 °C for 5 min and allowed to cool. Samples were separated by SDS/PAGE on a 10% TGX gel, transferred to a nitrocellulose membrane, and blocked for 1 h (5% milk in PBS/Tween). Blots were probed with a rabbit polyclonal anticaspase-3 antibody (Cell Signaling Technologies, 9662S, 1:1000 in 5% milk in PBS/Tween) overnight and goat antirabbit-antibody (Li-Cor Inc., 926-3221, 1:10 000 in 5% BSA in PBS/Tween) for 1 h.

Expression and Purification of TXN K72A Mutant

To produce a His-tagged K72A TXN protein, a QuikChange Lightning SiteDirected Mutagenesis Kit (Agilent Technologies, 210518) was used. A recombinant cDNA construct containing wild-type mammalian TXN in a pET 16B vector was obtained from Professor Michael Marletta. Mutagenesis was performed using the manufacturer's protocol with the following primers:

Forward: CTGGAATGTTGGCATGCATGCGACTTCACACTCTGAAGCA

Reverse: TGCTTCAGAGTGTGAAGTCGCATGCATGCCAACATTCCAG

The mutation was confirmed by DNA sequencing. Rosetta competent *E. coli* cells (Millipore Sigma, 70954–3) were then transformed with the plasmid and cultured to express the mutant in lysogeny broth and 0.1% ampicillin. Cultures were pelleted and lysed by probe sonication. Ni NTA Superflow resin (Qiagen, 30410) was used to purify the His-tagged mutant. The resin was loaded into a column, and the bacterial lysate was added. The column was washed 5 times with 1 mL of 10 mM imidazole. The His-tagged mutant TXN was eluted with 0.5 M imidazole. Purity was confirmed by SDS/PAGE and Coomassie staining. The purified protein was dialyzed in 10% glycerol in PBS overnight and stored at -80°C .

TXN Overexpression and qPCR Confirmation

To generate stable TXN overexpressing cells, a lentiviral plasmid in a pCMVSPORT6 vector containing human TXN was purchased from GE Healthcare Dharmacon Inc. and transfected into HEK293T cells using Lipofectamine 2000 (Life Technologies, 11668019). Lentivirus from culture medium was used to infect the target cell line with Polybrene, followed by selection of cells under $10\ \mu\text{g}/\text{mL}$ blasticidin for 3 days. Overexpression was confirmed via qPCR using the manufacturer's protocol for Fisher Maxima SYBR Green. Sequences of primers are as follows:

Thioredoxin forward: GTGAAGCAGATCGAGAGCAAG

Thioredoxin reverse: CGTGGCTGAGAAGTCAACTACTA

Cyclophilin forward: CCCACCGTGTCTTCGACATT

Cyclophilin reverse: GGACCCGTATGCTTTAGGATGA

Thioredoxin Activity Assay

A thioredoxin activity assay kit was purchased from Cayman Chemical Co. (20039). Samples were prepared in a 96-well black-walled plate. To each sample well, $54\ \mu\text{L}$ of assay buffer, human thioredoxin ($10\ \mu\text{L}$ of $0.2\ \mu\text{M}$ solution), human thioredoxin reductase ($10\ \mu\text{L}$ of $1.0\ \mu\text{M}$ solution), KEA1–97, and $5\ \mu\text{L}$ of NADPH (diluted according to kit instructions) were added. The plate was incubated at 37°C for 30 min. After incubation, $20\ \mu\text{L}$ of fluorescent substrate (diluted according to kit instructions) was added to each sample as quickly as possible. The plate was immediately placed in a SpectraMax i3 plate reader (Molecular Devices) and fluorescence was monitored over 1 h after 480 nm excitation and 520 nm emission. Reaction rates were plotted and compared.

Flow Cytometry Analysis of Cell Viability and Apoptosis

For the analysis of early and late stage apoptosis, cells were isolated and stained according to the instructions of the manufacturer. Briefly, media and trypsinized cells were pelleted by centrifugation at 500g for 5 min, washed once in PBS, and resuspended in binding buffer ($10\ \text{mM}$ HEPES/NaOH at pH 7.4, $140\ \text{mM}$ NaCl, $2.5\ \text{mM}$ CaCl_2) containing propidium iodide

(BD Biosciences) and FITC-conjugated Annexin V (BD Biosciences). Following a 15 min incubation, the cells were diluted with binding buffer to a final volume of 0.5 mL and the fluorescence measured using a BD Biosciences LSR Fortessa cytometer. FlowJo Software was used for all data analysis. The percentage of early apoptotic (Annexin V positive, propidium iodide negative) and late apoptotic (Annexin V positive, propidium iodide positive) cells was quantified ($n = 3$).

For the measurement of caspase-3/7 activity, 2 μM CellEvent Caspase-3/7 Green Detection Reagent (Invitrogen) was added to the media during the final 30 min of the treatment. Media and trypsinized cells were pelleted by centrifugation at 500g for 5 min, washed once in PBS, and resuspended in PBS. The fluorescence was measured using a BD Biosciences LSR Fortessa flow cytometer. FlowJo Software was used for data analysis, and the percentage of cells exhibiting active caspase-3/7 was quantified ($n = 3$). A t test was employed for all statistical analyses.

Supplementary Material

Refer to Web version on PubMed Central for supplementary material.

ACKNOWLEDGMENTS

This work was supported by the National Institutes of Health (R01 CA172667, R01 GM112948), American Cancer Society Research Scholar Award (RSG14-242-01-TBE), Department of Defense Breast Cancer Research Program Breakthroughs Award (CDMRP W81XWH-15-1-10050), the Novartis Institutes for BioMedical Research (NIBR), and the Novartis– Berkeley Center for Proteomics and Chemistry Technologies.

REFERENCES

- (1). Gangadhar NM, and Stockwell BR (2007) Chemical genetic approaches to probing cell death. *Curr. Opin. Chem. Biol.* 11, 83–87. [PubMed: 17174591]
- (2). Dixon SJ, and Stockwell BR (2009) Identifying druggable disease-modifying gene products. *Curr. Opin. Chem. Biol.* 13, 549–555. [PubMed: 19740696]
- (3). Smukste I, and Stockwell BR (2005) Advances in chemical genetics. *Annu. Rev. Genomics Hum. Genet.* 6, 261–286. [PubMed: 16124862]
- (4). Roberts AM, Ward CC, and Nomura DK (2017) Activitybased protein profiling for mapping and pharmacologically interrogating proteome-wide ligandable hotspots. *Curr. Opin. Biotechnol.* 43, 25–33. [PubMed: 27568596]
- (5). Weerapana E, Simon GM, and Cravatt BF (2008) Disparate proteome reactivity profiles of carbon electrophiles. *Nat. Chem. Biol.* 4, 405–407. [PubMed: 18488014]
- (6). Backus KM, Correia BE, Lum KM, Forli S, Horning BD, González-Pérez GE, Chatterjee S, Lanning BR, Teijaro JR, Olson AJ, Wolan DW, and Cravatt BF (2016) Proteome-wide covalent ligand discovery in native biological systems. *Nature* 534, 570–574. [PubMed: 27309814]
- (7). Roberts AM, Miyamoto DK, Huffman TR, Bateman LA, Ives AN, Heslin MJ, Akopian D, Contreras CM, Rape M, Skibola CF, and Nomura DK (2017) Chemoproteomic Screening of Covalent Ligands Reveals UBA5 as a Novel Pancreatic Cancer Target. *ACS Chem. Biol.* 12, 899. [PubMed: 28186401]
- (8). Shannon DA, Banerjee R, Webster ER, Bak DW, Wang C, and Weerapana E (2014) Investigating the proteome reactivity and selectivity of aryl halides. *J. Am. Chem. Soc.* 136, 3330–3333. [PubMed: 24548313]
- (9). Hacker SM, Backus KM, Lazear MR, Forli S, Correia BE, and Cravatt BF (2017) Global profiling of lysine reactivity and ligandability in the human proteome. *Nat. Chem.*, DOI: 10.1038/nchem.2826.

- (10). Ward CC, Kleinman JI, and Nomura DK (2017) NHSEsters As Versatile Reactivity-Based Probes for Mapping ProteomeWide Ligandable Hotspots. *ACS Chem. Biol.* 12, 1478. [PubMed: 28445029]
- (11). Lin S, Yang X, Jia S, Weeks AM, Hornsby M, Lee PS, Nichiporuk RV, Iavarone AT, Wells JA, Toste FD, and Chang CJ (2017) Redox-based reagents for chemoselective methionine bioconjugation. *Science* 355, 597–602. [PubMed: 28183972]
- (12). Mitchell DA, Morton SU, Fernhoff NB, and Marletta MA (2007) Thioredoxin is required for S-nitrosation of procaspase-3 and the inhibition of apoptosis in Jurkat cells. *Proc. Natl. Acad. Sci. U. S. A.* 104, 11609–11614. [PubMed: 17606900]
- (13). Bateman LA, Nguyen TB, Roberts AM, Miyamoto DK, Ku W-M, Huffman TR, Petri Y, Heslin MJ, Contreras CM, Skibola CF, Olzmann JA, and Nomura DK (2017) Chemoproteomics-enabled covalent ligand screen reveals a cysteine hotspot in reticulon 4 that impairs ER morphology and cancer pathogenicity. *Chem. Commun.* 53, 7234.
- (14). Zhao Q, Ouyang X, Wan X, Gajiwala KS, Kath JC, Jones LH, Burlingame AL, and Taunton J (2017) Broad-Spectrum Kinase Profiling in Live Cells with Lysine-Targeted Sulfonyl Fluoride Probes. *J. Am. Chem. Soc.* 139, 680–685. [PubMed: 28051857]
- (15). Kohnz RA, Roberts LS, DeTomaso D, Bideyan L, Yan P, Bandyopadhyay S, Goga A, Yosef N, and Nomura DK (2016) Protein Sialylation Regulates a Gene Expression Signature that Promotes Breast Cancer Cell Pathogenicity. *ACS Chem. Biol.* 11, 2131–2139. [PubMed: 27380425]
- (16). Louie SM, Grossman EA, Crawford LA, Ding L, Camarda R, Huffman TR, Miyamoto DK, Goga A, Weerapana E, and Nomura DK (2016) GSTP1 Is a Driver of Triple-Negative Breast Cancer Cell Metabolism and Pathogenicity. *Cell Chem. Biol.* 23, 567–578. [PubMed: 27185638]
- (17). Weerapana E, Wang C, Simon GM, Richter F, Khare S, Dillon MBD, Bachovchin DA, Mowen K, Baker D, and Cravatt BF (2010) Quantitative reactivity profiling predicts functional cysteines in proteomes. *Nature* 468, 790–795. [PubMed: 21085121]
- (18). Wang C, Weerapana E, Blewett MM, and Cravatt BF (2013) A chemoproteomic platform to quantitatively map targets of lipid-derived electrophiles. *Nat. Methods* 11, 79–85. [PubMed: 24292485]
- (19). Roberts AM, Miyamoto DK, Huffman TR, Bateman LA, Ives AN, Akopian D, Heslin MJ, Contreras CM, Rape M, Skibola CF, and Nomura DK (2017) Chemoproteomic Screening of Covalent Ligands Reveals UBA5 As a Novel Pancreatic Cancer Target. *ACS Chem. Biol.* 12, 899–904. [PubMed: 28186401]

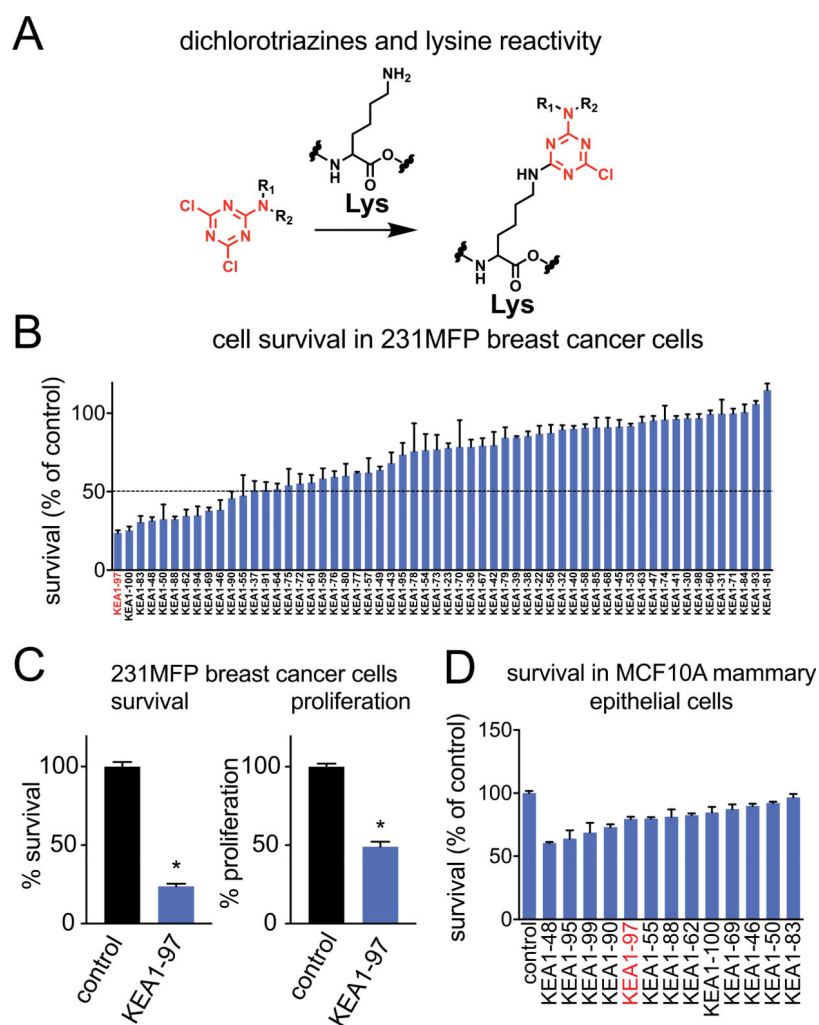


Figure 1. Screening of dichlorotriazine library in breast cancer cells. (A) Dichlorotriazines have been shown to have preferred reactivity with lysines. A library of 58 dichlorotriazines was synthesized. (B) This library was screened ($10\ \mu\text{M}$) in 231MFP breast cancer cells for impairments in serumfree cell survival after 48 h compared to ACN-treated controls. The top hit from this screen was KEA1-97. Detailed data can be found in Table S1. (C) KEA1-97 ($10\ \mu\text{M}$) impairs 231MFP serum-free cell survival and proliferation after 48 h. (D) Counterscreen of hits in MCF10A cells ($10\ \mu\text{M}$, 48 h). Data are shown as average \pm SEM, $n = 3/\text{group}$. Significance is expressed as $*p < 0.05$ compared to control.

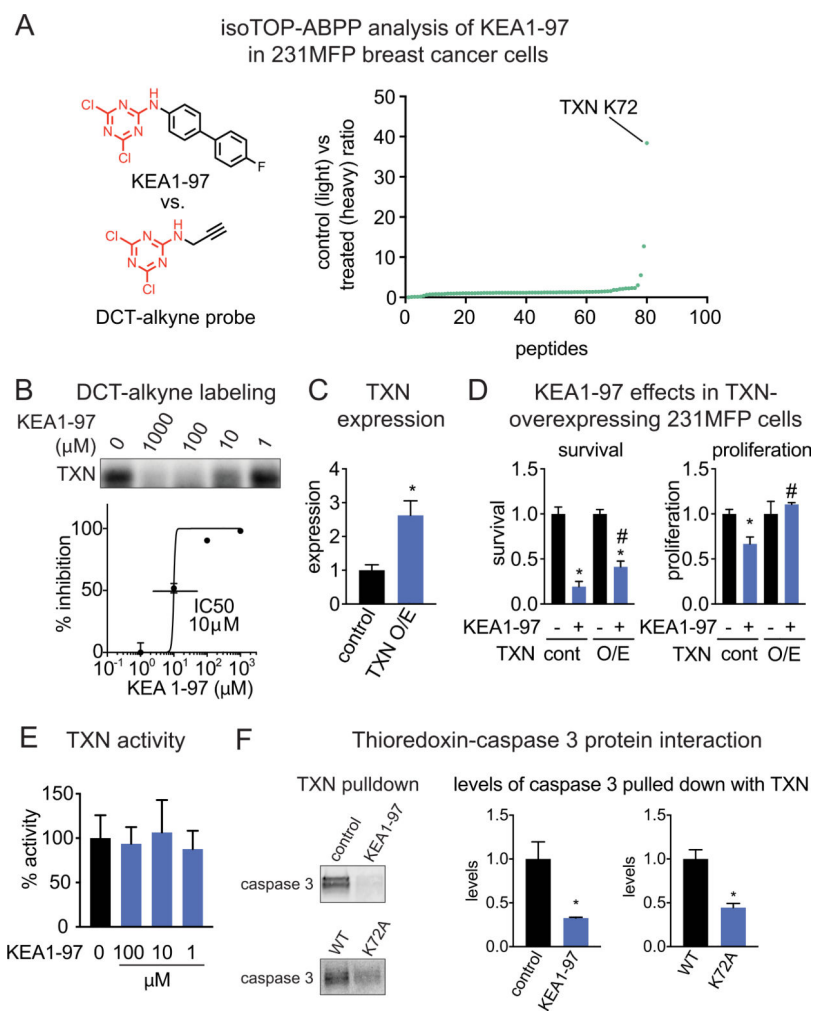


Figure 2. KEA1-97 targets thioredoxin. (A) IsoTOP-ABPP analysis of KEA1-97 (10 μM) in 231MFP breast cancer proteomes using DCT-alkyne probe. 231MFP breast cancer proteomes were pretreated with acetonitrile vehicle or KEA1-97 prior to labeling with DCT-alkyne (100 μM) for 1 h, followed by CuAAC-mediated appendage of light or heavy enrichment handles, and analysis of eluted probe-modified peptides by LC-LC/MS/MS. Structures of KEA1-97 and DCT-alkyne are shown on the left. Shown on the right are isotopically light (acetonitrile-treated) to heavy (KEA1-97-treated) probe-modified peptide ratios for peptides identified in two out of three biological replicates. Detailed data can be found in Table S2. (B) Gel-based ABPP studies showing competition of KEA1-97 against DCT-alkyne labeling (10 μM) of pure human TXN. Shown is a representative gel and a dose-response curve. (C) TXN expression in GFP control or TXN-overexpressing 231MFP cells as assessed by qPCR. (D) Cell survival of 231MFP control or TXN-overexpressing cells treated with acetonitrile vehicle or KEA1-97 (10 μM) for 24 h as assessed by Hoechst stain. (E) TXN activity assay. (F) Disruption of TXN interaction with caspase 3 upon treatment with KEA1-97 or mutation of TXN K72 to alanine. In the upper blot and left bar graph, pure His-tagged TXN and caspase 3 were preincubated with acetonitrile or KEA1-97 (100 μM) prior to anti-His pull-down, SDS/PAGE, and blotting for caspase 3. In the lower blot and right bar graph, pure

His-tagged TXN or TXN K72A mutant protein and caspase 3 were preincubated, subjected to anti-His pull-down, SDS/PAGE, and blotting for caspase 3. Data in B–E are shown as average \pm SEM; data in A–F are $n = 3$ /group. Significance is expressed as * $p < 0.05$ compared to controls and # $p < 0.05$ compared to KEA1–97-treated controls.

Author Manuscript

Author Manuscript

Author Manuscript

Author Manuscript

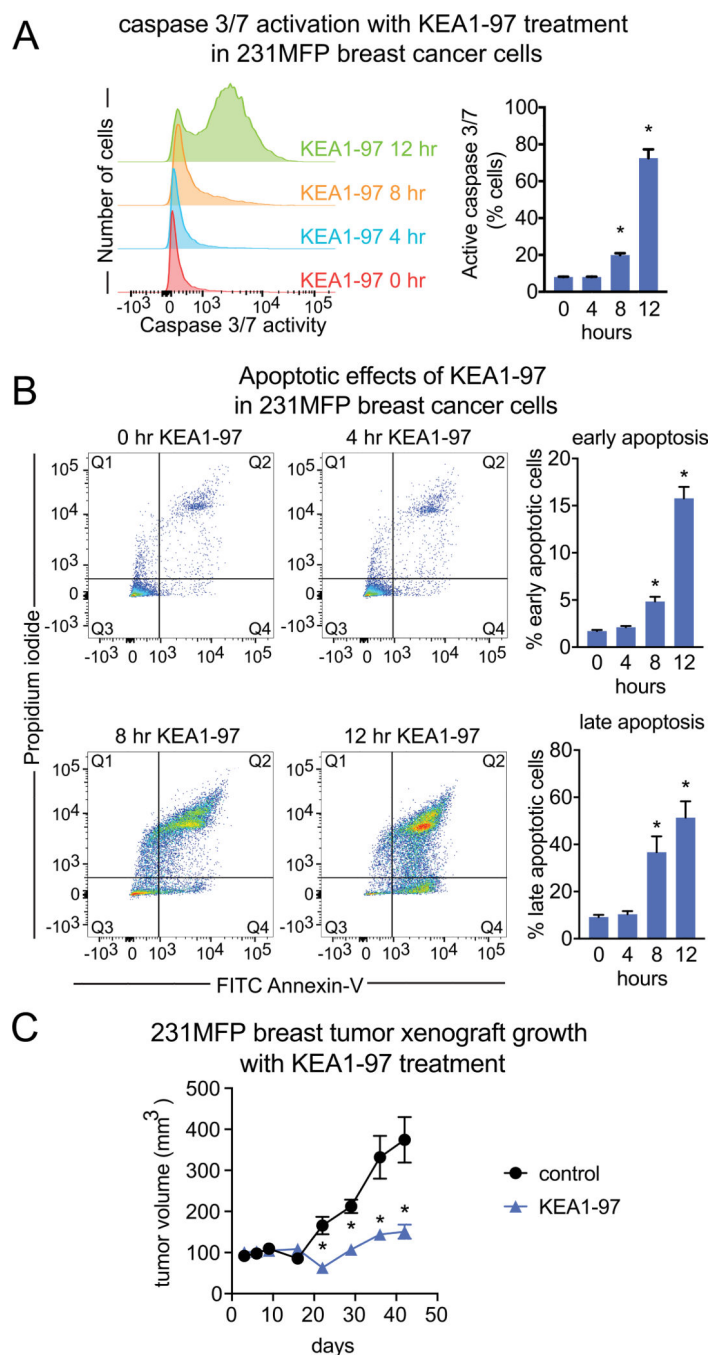


Figure 3. Apoptosis and antitumorigenic effects induced by KEA1-97 in 231MFP breast cancer cells. (A) Caspase 3/7 activation using a CellEvent Caspase 3/7 Green Detection Reagent. (B) KEA1-97 (10 μ M) induces apoptosis in 231MFP breast cancer cells assessed by propidium iodide and FITC Annexin-V staining and quantified by flow cytometry. (C) KEA1-97 treatment (5 mg/kg ip once per day) was initiated 16 days after the initiation of 231MFP tumor xenografts in immune-deficient SCID mice. Data in A–C are shown as average \pm

SEM. Data are $n = 3$ /group in A and B, and $n = 8$ mice/group in C. Significance is expressed as $*p < 0.05$ compared to control.